JOURNAL OF PROPULSION AND POWER
Vol. 9, No. 3, May–June 1993

Computational Study of Advanced Exhaust System Transition Ducts with Experimental Validation

C. Wu,* S. Farokhi,† and R. Taghavi‡
University of Kansas, Lawrence, Kansas 66045

A subsonic, three-dimensional parabolized Navier-Stokes code is used to construct stall margin design charts for optimum-length advanced exhaust systems' circular-to-rectangular transition ducts. Computer code validation has been conducted to examine the capability of wall static pressure predictions. The comparison of measured and computed wall static pressures indicates a reasonable accuracy of the PNS computer code results. Computations have also been conducted on 15 transition ducts, 3 area ratios, and 5 aspect ratios. The three area ratios investigated are constant area ratio of unity, moderate contracting area ratio of 0.8, and highly contracting area ratio of 0.5. The degree of mean flow acceleration—i.e., the area ratio of the duct—is identified as a dominant parameter in establishing the minimum duct length requirement. The effect of increasing aspect ratio in the minimum length transition duct is to increase the length requirement, as well as to increase the mass-averaged total pressure losses.

Nomenclature

A_e/A_i = area ratio: ratio of duct exit area to duct inlet area
AR = aspect ratio: ratio of duct width to height at the exit plane
a = semimajor axis of the superelliptic cross section
b = semiminor axis of the superelliptic cross section
C_{fg} = nozzle gross thrust coefficient, $\equiv F_{g,\text{actual}}/F_{g,\text{ideal}}$
D = inlet diameter, in.
F_g = gross thrust
L/D = length ratio: ratio of duct length to inlet diameter
M = Mach number
n = superelliptic exponent
P = static pressure, psia
R = inlet radius
Re = Reynolds number
T = static temperature, °R
x = distance along the axis of the transition duct, in.
y, z = coordinates in the plane of the duct cross section

Subscripts
e = exit
i = inlet
t = total or stagnation
ws = wall static

Introduction

MODERN fighter aircraft are required to be super maneuverable at subsonic, transonic, and supersonic speeds, as well as to have stealth characteristics. Modern aircraft engines are therefore designed to fulfill these tasks. One important feature of modern aircraft engines' advanced exhaust systems is their extensive use of transition ducts. For example, the F-117 Stealth Fighter, the B-2 Stealth Bomber, and the YF-22 Advanced Tactical Fighter all have exhaust systems in which the ducts connecting the turbine exit plane to the nozzle exit undergo a continuous transition from round to rectangular geometry—the so-called "transition duct." The use of rectangular nozzles for thrust vectoring and reversal can improve the agility, maneuverability and flight controllability of the aircraft. Additional advantages of rectangular nozzles are noted in their capability of masking the engine hot section and in their reduced infrared signature due to the enhanced mixing of the hot exhaust gases with ambient air.[1] On the negative side, a transition duct will generate recirculation zones around the interior corners and three-dimensional flow separation can also occur due to rapid local flow diffusion in a three-dimensionally varying flow passage. Flow separation and recirculation zones all result in "usable" energy loss, which must be minimized to achieve a high C_{fg}. With optimum-length nozzles, the weight of an aircraft exhaust system will also be minimized, which is an inherent design goal for all aircraft. Investigation of minimum-length transition ducts with no flow separation is therefore of utmost practical importance.

Several experimental and computational investigations covering transition ducts have been conducted in the past. A few important works in this area are briefly noted here. The earliest experimental investigation of transition ducts was performed by Mayer[2] over half a century ago. Mayer's research involved both round-to-rectangular and rectangular-to-round ducts of neutral diffusion; i.e., area ratio of unity. Low-speed, fully developed, turbulent inlet profiles were examined at inlet Reynolds number of 192,000, based on inlet hydraulic diameter. Mayer's experiments showed that the secondary flow pattern emerging from a round-to-rectangular transition duct was significantly stronger than the pattern from a rectangular-to-round transition duct. The formation of corner vortices in the streamwise direction is weakened, or smeared off, by rounding off the corners from rectangular-to-round transition. The transition from round-to-rectangular cross section in a duct, however, provides the mechanism for feeding energy from the primary flow to generate a secondary flow pattern.

Burley et al.[3] experimentally investigated five nonaxisymmetric, circular-to-rectangular transition ducts, all with exit aspect ratio of 6.33. Four configurations were of constant area, while the fifth configuration was an accelerating duct of area ratio 0.75. The geometry of transition-duct cross sections

Received May 7, 1992; presented as Paper 92-3794 at the AIAA/SAE/ASME/ASEE 28th Joint Propulsion Conference, Nashville, TN, July 6–8, 1992; revision received Dec. 26, 1992; accepted for publication Jan. 6, 1993.

*Graduate Research Assistant; currently with United Technologies, USBI, P.O. Box 1900, Huntsville, Alabama 35807. Member AIAA.

†Professor of Aerospace Engineering and Director of Flight Research Laboratory. Senior Member AIAA.

‡Assistant Professor of Aerospace Engineering. Member AIAA.

was described by a family of superellipses. Nozzle performance parameters such as discharge coefficient and thrust ratio (defined as the ratio of actual to ideal gross thrust) and wall static pressure data are presented in Ref. 3. The effect of duct length on discharge and thrust coefficients is also presented. The shortest configuration having a length-to-diameter ratio of 0.5 was badly stalled, as observed by its lower discharge and thrust coefficients. The "best" nozzle performance among the configurations tested in Ref. 3 was recorded for a transition duct with length ratio (i.e., L/D) of 1, which had a more gentle wall slope and better boundary-layer behavior. Effect of transition duct sidewall shape on discharge and thrust coefficients was also explored in Ref. 3. Nearly identical discharge and thrust coefficients were measured for both straight and cubic sidewall geometries. The straight sidewall duct slightly outperformed the cubic sidewall transition duct primarily due to a lower maximum wall curvature. Also investigated was the effect of duct contraction on discharge and thrust coefficients. Two configurations with exit-to-inlet area ratios of 1.0 and 0.75 and length ratios of 1.0 and 0.75 were considered. The transition duct with accelerating mean flow exhibited a higher discharge coefficient, by about 1.8%, over the neutral-diffusion duct. Favorable streamwise pressure gradient in the accelerating duct led to thinner boundary layers and was deemed responsible for a higher discharge coefficient. An improved gross thrust coefficient was not noticeable except at nozzle pressure ratios (NPR) above 4. In general, with the help of favorable pressure gradient, accelerating ducts with shorter lengths are capable of outperforming neutral-diffusion ducts with longer lengths.

Patrick and McCormick[4] conducted a detailed laser velocimeter investigation of two circular-to-rectangular transition ducts at low subsonic speeds. The straight centerline ducts were of constant area transition with aspect ratios of 3 and 6, corresponding L/D of 1.0 and 3.0, respectively. It was found that the evolution of corner vortices was much more profound for the high-aspect-ratio duct, as compared to the shorter, low-aspect-ratio duct. Neither of the two transition ducts exhibited any sign of flow separation at the measurement planes.

From the review of experimental literature, one may find that the topic of minimum-length transition ducts has not been the main objective of earlier investigations. As there are infinitely many ways for a duct to achieve transition from a circular to a rectangular geometry, it is neither economical nor practical to find the best transition geometry and the optimum length by testing each duct experimentally. However, computational techniques have been applied to the fluid dynamic analysis of transition-ducts. A potential inviscid flow analysis using panel method code (MCAERO) was performed by Burley et al.[3] The features of viscous-dominated flow near the walls were beyond the scope and capability of the inviscid (and potential) code used in Ref. 3. Consequently, the surface pressures could not be predicted accurately by Burley et al.[3]

Anderson[5] has established a linear stall-margin design chart for the round-to-rectangular transition ducts, utilizing a three-dimensional viscous code (PEPSI-G). The design chart is for straight centerline, neutral diffusion, and accelerating ducts of constant area ratio 1.0 and contracting, exit-to-inlet area ratio 0.633, respectively. The exponent of superelliptic cross sections, defining the "roundness" of the corners in Anderson's investigation, was 2 at the inlet section and limited to 10 at the exit plane. This represented a first attempt in applying CFD techniques to predicting stall-margin for transition ducts.

Farokhi et al.[1] investigated the optimum-length circular-to-rectangular transition ducts by using PEPSIG-G as an analysis code. The cases of straight centerline, two-dimensional offset with neutral diffusion, and highly contracting ducts of exit-to-inlet area ratio 0.5 were computed. The aspect ratios considered were 1.3 and 5.1 for neutral diffusion ducts, 2.56 and 10.19 for accelerating ducts, respectively. Stall-margin design charts for optimum-length transition dusts were established and the mass-averaged total pressure loss was calculated. Detailed results and discussion can be found in Ref. 1.

In the present article, the PEPSI-G code is again used as a computational tool. For the purpose of code validation, both experiments and computations were conducted for a specific transition duct. The computational results are compared with experimental data.[6] The comparison shows reasonable accuracy in wall static pressure predictions. Finally, computations of transition ducts with straight centerline having three area ratios, each with five different aspect ratios, were also performed. Based on the computational results, stall-margin design charts of optimum-length transition ducts, as well as the associated mass-averaged total pressure loss, are constructed.

Computer Code and Its Validation

Criteria of Choosing the Computer Code

The viscous-dominated internal flowfield of a round-to-rectangular transition duct is complicated in the following aspects: the corner vortices may be generated due to the transitioning from round-to-rectangular geometry inside the duct; the flow experiences frictional losses due to presence of the walls. Potential flow solvers, e.g., panel methods, and Euler solvers are not adequate to treat the problem at hand since they neglect the effects of vorticity and viscosity. Furthermore, it is the inherent nature of the viscous flow in a corner—i.e., merging of the two boundary layers, and the significant lateral extent such as cross-stream diffusion of the viscous zone into the core flow—that will prevent the use of conventional boundary-layer approach. Through the above process of elimination, the time-averaged Navier-Stokes codes are identified as the only suitable analysis tool for the purpose of this study. The ideal approach for computation of three-dimensional flows in transition ducts would require numerical solutions of the full Navier-Stokes equations which are fully elliptic and demand tremendous CPU time and memory requirements. Although these are feasible, it is still extremely expensive to do so, even with the state-of-art numerical technology and today's most powerful super computers. As an alternative, the PEPSI-G, a three-dimensional, subsonic, parabolized Navier-Stokes (PNS) flow solver is utilized as the computational tool. The code offers a space (i.e., streamwise) marching capability instead of iterations required in full Navier-Stokes (FNS) codes. The computer running time for a PNS code is equivalent to one iteration of the FNS code, which translates into considerable saving in the CPU time and computer memory requirements. The main drawback of PNS codes is their inability to march through massive flow separations. However, the purpose of this study is to establish optimum-length transition ducts which will not encounter massive flow separations. Based on these considerations, PEPSI-G code suits the purpose of this investigation very well.

Brief Description of the Computer Code

The PEPSI-G code was initially developed by Levy et al.[7,8] based on the theoretical formulation of Briley.[9] The PEPSI-G is the acronym for parabolic equations procedure solved implicitly—generalized coordinates code. Although details of the analysis and the computer program may be found in Refs. 7–12, a brief outline of the computational methodology is presented here for the sake of completeness.

The flowfield is divided into one streamwise (primary) and two transverse (secondary) directions, with the duct centerline identifying the primary flow direction. The viscous streamwise marching solution is primarily enabled through neglecting the streamwise diffusion terms in the governing equations. The physically required ellipticity of the flowfield is, however, introduced by a potential flow solver to the viscous code. The viscous solution requires the pressure field information supplied by a potential flow solver. The turbulence model in PEPSI-G is based on the mixing-length hypothesis. The meth-

odology to treat separated wall flows in the code was developed by Reyhner and Flugge-Lotz[13] and is referred to as "FLARE" approximation in the literature. The procedure simply keeps the primary flow always marching in the streamwise direction. In other words, if reverse flow is detected in the marching direction, it is then substituted by a small positive value to keep the primary flow always positive. This is the main reason why parabolized codes cannot handle the flow separation phenomenon in a more physically meaningful way.

The geometries of transition ducts are described by centerline shape in primary flow direction and superellipse equation, $(y/a)^n + (z/b)^n = 1$, in transverse direction. The corner shape is described by the exponent of the superelliptic cross section n, which varies from 2 to 10 in PEPSI-G code. If $a = b$, then $n = 2$ represents a circular cross section, and $n = 10$ describes a square cross section with small round corners. A larger value of n in the superellipse equation will construct a square or a rectangle with very sharp corners, which is beyond the scope and capability of the code.

Computer Code Validation

Widespread acceptability of the results of a computer code is essentially based on the success of the code validation efforts performed by means of bench mark experiments. The PEPSI-G code has been extensively validated by bench mark experiments performed in the industry, NASA, and universities. References 14–19 exemplify the sources of bench mark experimental data and the computational validation efforts. However, most of the comparisons made between experimental data and the computational results are mainly velocity profiles and contour plots of the flow in either circular or square cross section ducts. From manufacturing and performance points of view, the wall static pressure distributions and total pressure loss are more important information for the engineers. However, this information is rarely reported in the open literature. Therefore, in this study, the computer code is validated for the wall static pressure prediction in a transition duct.

The geometry of the circular-to-rectangular transition duct is shown in Fig. 1. It is a straight centerline, slightly accelerating transition duct with R of 18.32 in., slightly contracting area ratio of 0.95, aspect ratio of 3.0, and length ratio of 1.03. The test inlet flow conditions are $M = 0.25$, $T_i = 2600°R$, and $P_i = 50$ psia. The inlet Reynolds number based on inlet radius is 2,700,000. The wall static pressure was measured in the streamwise and circumferential direction at $x/D = 0.1$, 0.3, 0.5, 0.7, and 0.9.

The numerical computations were performed by the authors at the University of Kansas, using CRAY X-MP super computer at NASA Lewis Research Center by way of telnet access. Some necessary modifications in the geometry of the computational model were made to adapt the computer code's acceptability of the geometry. Figure 2 presents the comparison between the exact and modified geometries for this particular duct. The main criterion for modification was to keep the computational geometry as close as possible to the test model, yet acceptable by the computer code. From parts a and b of Fig. 2, one notes that the shapes of the sidewall and the top wall, referred to as "horizontal cut a" and "vertical cut b," are identical between the test and the computational model. The main difference is in the corner shape distribution, which is referred to as "exponential n" in Fig. 2. The duct exit plane of test model was manufactured to a rectangular shape with extremely sharp corners; i.e, n is of 150, and the change of corner shape follows a steep exponential distribution, as shown in part a of Fig. 2. However, sharp corners and very steep gradients result in numerical discontinuities which prove disastrous for the convergence of the computation. Hence, the corner shape distribution has been modified to a certain degree; i.e., corners are slightly rounded up. For example, the maximum of the exponent index n is set to 10 for the computational model instead of 150 for the test model. This means that the corners of the rectangular duct cross section have been "rounded off" to some extent. Another major modification is made near the duct exit, where the first derivative of the corner shape distribution is set to nearly zero for the sake of the computational convergence. These modifications result in a slight change in transition duct area distribution but are still within the allowable design criterion.

A 100 × 100 computational grid was used in the cross plane, and 919 stations in the streamwise direction with dense grid packing near the walls. This is mainly due to the specified geometry, especially the exponential distribution of the corner shape. It took a total of 3.9 CPU hours on CRAY X-MP to complete the calculations in our duct. No flow separation has been detected in the transition duct, which is in agreement with the experimental measurements. The main computational results are presented in Figs. 3–5. Figures 3 and 4 show the comparison between the experimentally measured wall static pressure data and the computational results in streamwise and circumferential directions, respectively. The comparison shows a reasonable agreement in wall static pressure

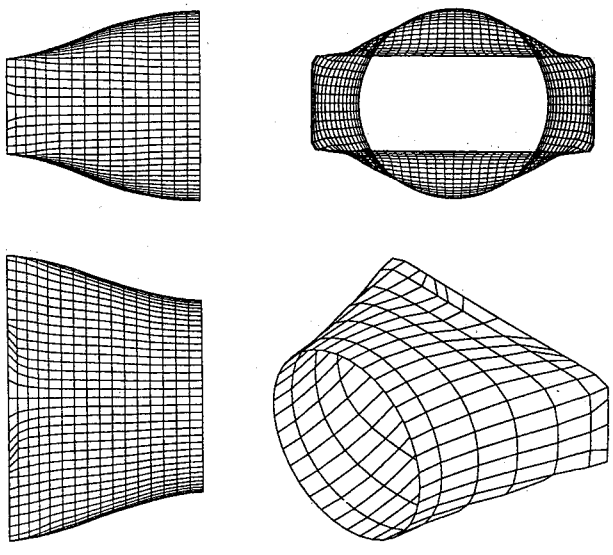

Fig. 1 Computational geometry of the transition duct; $L/D = 1.03$, $AR = 3.0$, $A_e/A_i = 0.95$.

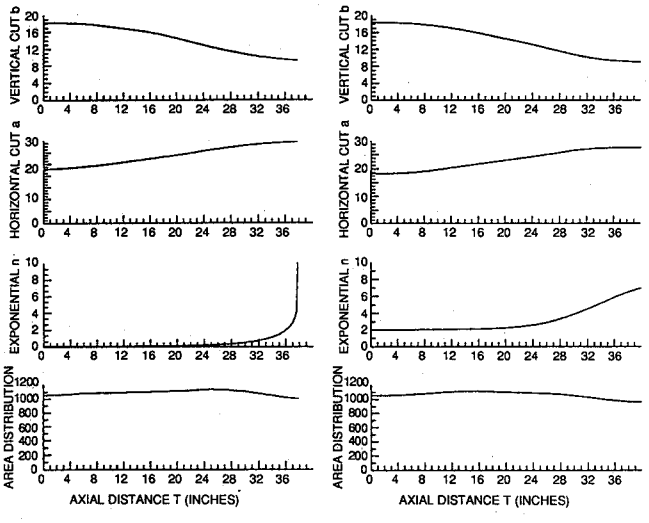

Fig. 2 Comparison between the exact geometry for experiment and the modified geometry for computation of transition duct; $L/D = 1.03$, $AR = 3.0$, $A_e/A_i = 0.95$.

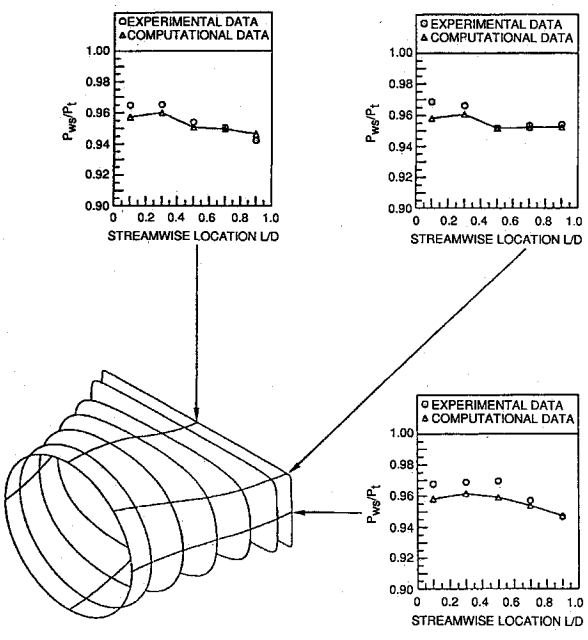

Fig. 3 Comparison between the experimental wall static pressure data in the streamwise direction and the CFD results.

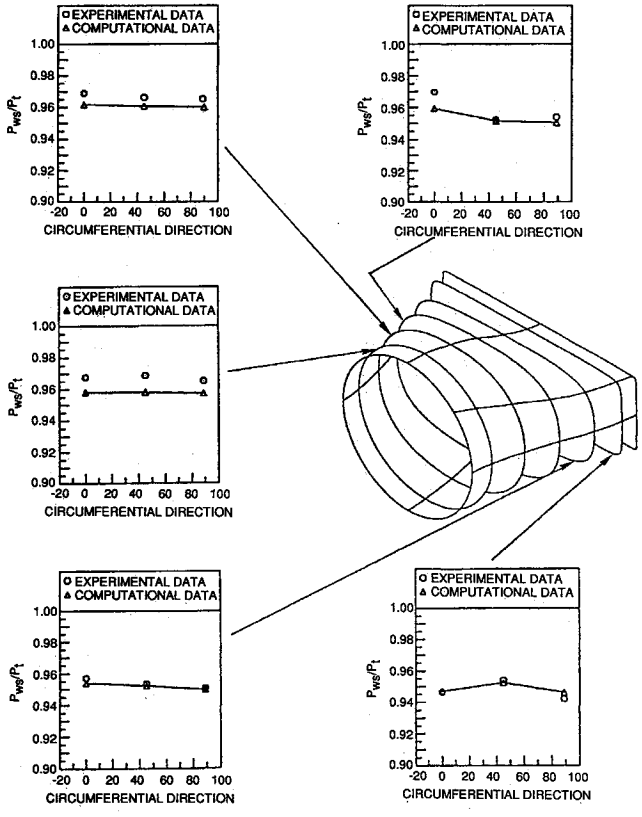

Fig. 4 Comparison between the experimental wall static pressure data in the circumferential direction and CFD results.

predictions by PEPSI-G code. Figure 5 demonstrates the streamwise velocity contours and secondary flow velocities at five locations within the transitions duct where wall static pressure measurements were made. It gives a general flow picture within the transition duct, which is usually not available from experimental measurements. Overall, the computer code validation is successful, and the parabolized Navier-Stokes code proved to be capable of predicting wall static pressure distribution in a complex geometry.

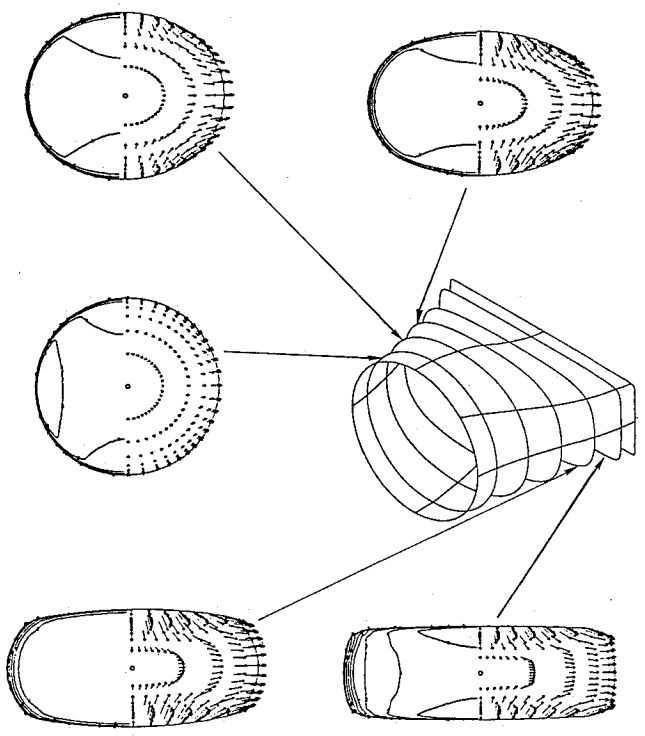

Fig. 5 Streamwise velocity contours and secondary velocities in the transition duct.

Stall Margin Design of Optimum-Length Transition Ducts

Computational Matrix

Upon successful completion of the computer code validation, computations for a matrix of transition ducts have been performed to construct the optimum-length transition ducts with no flow separation. The matrix included transition ducts of three area ratios, each with five different aspect ratios: $A_e/A_i = 1.0$ (neutral diffusion ducts) with $AR = 1.3, 3.0, 5.1, 7.0$, and 10.0; $A_e/A_i = 0.8$ (moderate contracting ducts) with $AR = 1.3, 3.0, 5.1, 7.0$, and 10.0; and $A_e/A_i = 0.5$ (highly contracting ducts) with $AR = 1.0, 2.6, 5.0, 7.0$, and 10.2. The inlet radius is set to 18.32 in., and the inlet flow conditions are the same as the test flow conditions noted earlier.

A restriction was imposed on the area distribution variations from the inlet-to-outlet planes of less than 10%. On the exponent distribution of the superelliptic shapes, the initial value of 2 was raised to a maximum value of 10 at the exit. Higher n values did not permit a converged solution by the code. The shapes of horizontal and vertical cuts are nearly cubic with about 50% duct length inflection points for the accelerating ducts.

Computation of Stall Margin

To establish "stall margin" in a transition duct of minimum length using a computational code is a complicated task. The complications arise from 1) the physics of three-dimensional flow separation which is neither amenable to the streamwise "marching" philosophy of a PNS code nor captured by a simple mixing-length approach of turbulence modeling; and 2) code convergence problems associated with steep geometrical gradients which may reflect the inadequacies of the numerical algorithm rather than the physical flow separation in the duct. Having stated the above concerns at the outset, we proceed to investigate the internal fluid mechanics of several transition ducts, near or beyond stall, as viewed by a PNS code. Although the exact separation point, reattachment length, and lateral extent of the three-dimensional separation zone

are/is not accurately predicted by the PNS code, the trends in minimum-length requirements are of value.

The cases studied for the neutral diffusion ducts are summarized in Fig. 6. To arrive at the minimum-length transition duct by using an analysis code in a successive manner, the initial calculation was performed for a rather conservative length ratio of 2 with aspect ratio of 1.3. No computational problems were encountered, since the flow remained fully attached and well behaved. Subsequently, the duct length was reduced to a shorter length ratio of 1, and a small flow separation was detected. The "small separation" is defined as the condition where a few flow separation points are found inside the transition duct during the computation, but these separations become reattached later and do not cause any computational problems. In the larger aspect ratio cases, the calculations were performed for aggressive choices of length ratios. For example, the calculation of neutral diffusion transition duct of $AR = 3$ was started at $L/D = 1.25$ and small flow separation was detected. By further reduction of the duct length, massive flow separation was encountered. The "massive separation" is defined as the flow undergoing a large, unrecoverable separation which poses a fluid mechanics problem for a PNS code and does not yield a solution. The optimum-length stall margin of neutral diffusion ducts is presented in the top plot of Fig. 6, and the "exact" stall margin, as viewed by PEPSI-G, should be on or slightly above the curve depicted by square symbols. We also note a nonlinear relationship between the exit aspect ratio and the minimum duct length requirements.

The cases studied for the moderate contracting transition ducts of area ratio 0.8 are summarized in the middle panel of Fig. 6. The minimum-length stall margin is clearly demonstrated by the symbols, where the circles represent attached flow, and the squares portray the flow with small separation. The exception is the case of $AR = 7.0$ at $L/D = 2.5$, for which the duct experienced massive separation instead of the small separation which might be expected. Again, we note a nonlinear variation of the minimum length requirement with the duct exit aspect ratio. In comparison to a neutral-diffusion duct (i.e., top panel of Fig. 6), the optimum-length requirement for the accelerating duct (of area ratio 0.8) is lower.

The other cases summarized in the bottom panel of Fig. 6 are the highly accelerating transition ducts with contracting area ratio of 0.5. In the cases of both $AR = 1.0$ and $AR = 2.6$, the calculated results show no flow separation at length ratio of 1.0. By further reducing the length ratios to $L/D = 0.8$ and 0.9, respectively, numerically indicated massive flow separations were encountered. The same experience repeated for the ducts with $AR = 5.0$ and $L/D = 1.5$, $AR = 7.0$ and $L/D = 1.75$, and $AR = 10.2$ and $L/D = 2.0$. The combination of high AR and a short L/D, imposes very steep gradients in the streamwise and cross flow directions which result in massive flow separations. As noted earlier, these are beyond the abilities of a PNS code. The numerically indicated optimum-length transition duct again follows a nonlinear relationship with the duct exit aspect ratio in the case of $A_e/A_i = 0.5$. However, the nonlinearity is less steep for the accelerating ducts than for the neutral-diffusion transition duct. The reader is cautioned that the PNS-indicated minimum length for a transition duct may be significantly "longer" than the physically required length of the same transition duct with no separation.

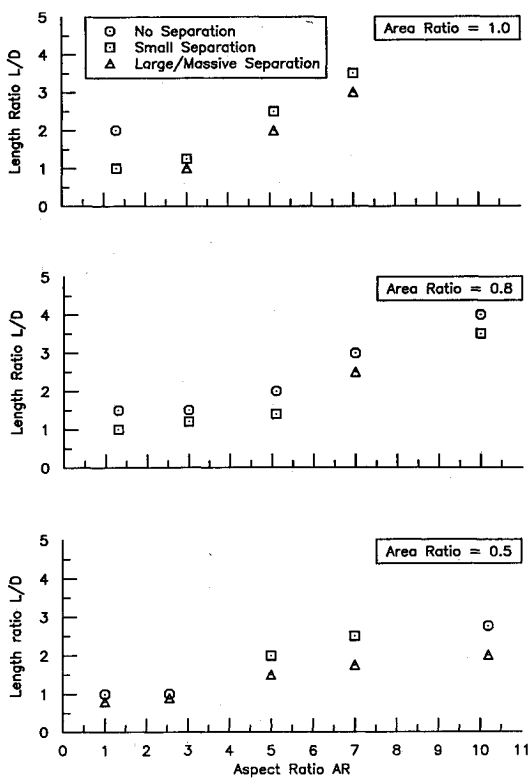

Fig. 6 Calculated stall margin for constant area and contracting transition ducts.

Viscous and Secondary Flow Losses

The flow losses inside a straight centerline transition duct are both the result of the integral of frictional drag on the wall and the kinetic energy loss due to the flow rotation in the cross plane. The effects of viscous and secondary flow losses in an adiabatic duct manifest themselves in the form of total pressure loss. The mass-averaged total pressure loss is defined as

$$\text{Total pressure loss} = \frac{\bar{P}_{t,\text{inlet}} - \bar{P}_{t,\text{exit}}}{\bar{P}_{t,\text{inlet}}} \tag{1}$$

The total pressure loss in the transition ducts, in terms of duct L/D and three different area ratios, is plotted in Fig. 7. The top plot in this figure shows the results of constant area transition ducts at four different aspect ratios. The total pressure

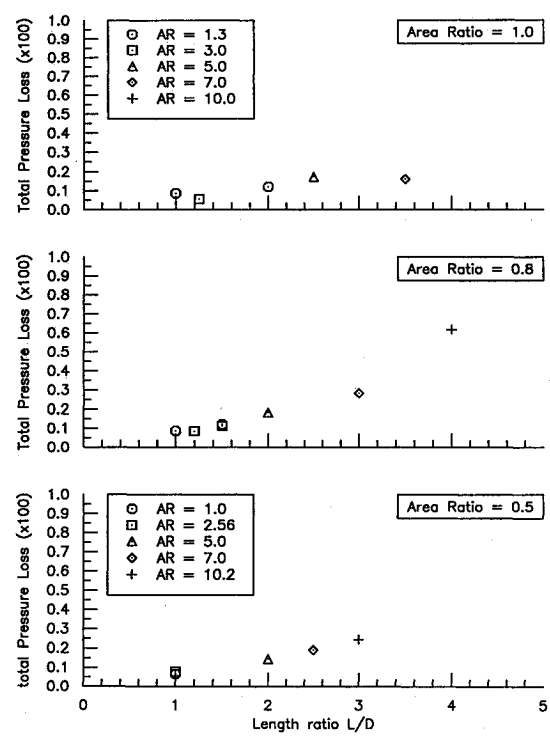

Fig. 7 Mass-averaged total pressure loss in constant area and contracting ducts with different length and area ratios.

loss at $L/D = 3.5$ and $AR = 7.0$ seems to be slightly lower than the total pressure loss at $L/D = 2.5$ and $AR = 5.1$. This consitutes an anomalous behavior. However, in light of very small numbers involved (i.e., hundredths of 1%) and the computational accuracy, this behavior may be explained. In the cases of moderate and high accelerating ducts (i.e., $A_e/A_i = 0.8$ and $A_e/A_i = 0.5$, respectively), the trends of mass-averaged total pressure loss follow our expectations; i.e., increase with aspect ratio and length ratio. In general, at the same length ratio, the duct with higher aspect ratio has higher "mean" total pressure loss. This is mainly caused by an increase of kinetic energy of the secondary flow in the cross plane. However, the dominant total pressure loss mechanism in a transition duct arises from the viscous frictional effects. This point is readily verified by examining the data in Fig. 7. Again, the reader is alerted to the accuracy of these loss estimations which stem from a reduced Navier-Stokes set of equations and a simple mixing-length-based turbulence modeling.

Conclusions

An existing PNS computer code has been applied to a "real" design and analysis environment. The comparison of wall static pressures, in measurement and computation, has proved the reasonable accuracy in PNS computational capabilities. Some modifications in the computational geometries were deemed necessary to proceed with PNS computations. The viscous flow in transition ducts with straight centerline and area ratios of 1.0, 0.8, and 0.5 at five different aspect ratios were calculated. Based on the computational results, three charts for the optimum-length transition ducts, as indicated by a parabolized Navier-Stokes code, were constructed. The corresponding mass-averaged total pressure losses generally ranged in tenths of 1% and increased with both aspect ratio and length ratio. The transition duct area ratio was found to have a significant effect on the duct length requirement as well as on the total pressure losses. The optimum-length transition ducts with higher contraction area ratio exhibited shorter duct lengths and lower total pressure losses as compared to moderate contraction area ratio and neutral diffusion ducts of similar aspect ratio. The effect of mean streamwise flow acceleration is noted to reduce the duct length requirement.

Acknowledgments

The financial support for this study was provided by GE Aircraft Engines under P.O. 200-14BE-14U11696. Access to CRAY X-MP super computer and technical support were provided by NASA-Lewis Research Center under Cooperative Agreement NAG 3-841. The authors are indebted to their colleagues Don Dusa, Don Dietrich, and David Evans of the GE-Aircraft Engines, and Charles Towne and Bernhard Anderson of the NASA Lewis Research Center, for their financial and technical support. The efforts of Gary Cheng and Wen Sheu in transition duct computations are both acknowledged and appreciated.

References

[1]Farokhi, S., Sheu, W. L., and Wu, C., "On the Design of Optimum-Length Transition Ducts with Offset: A Computational Study," *Computers and Experiments in Fluid Flow*, edited by G. M. Carlomagna and C. A. Brebbia, Springer-Verlag, Berlin, 1989, pp. 215–228.

[2]Mayer, E., "Einfluss der Querschnittverformung auf die Entwicklung der Geschwindigkeits—und Druckverteilung bei turbulente Stroemungen in Rohren," VDI-Forschungsheft 389, March/April 1938; see also NACA TM-903, Aug. 1939.

[3]Burley, J. R., Bangert, L. S., and Carlson, J. R., "Static Investigation of Circular-to-Rectangular Transition Ducts for High-Aspect-Ratio Nonaxisymmetric Nozzles," NASA TP-2534, March 1986.

[4]Patrick, W. P., and McCormick, D. C., "Laser Velocimeter and Total Pressure Measurements in Circular-to-Rectangular Transition Ducts," UTRC Rept. 87-41, June 1988.

[5]Anderson, B. H., private communication, NASA Lewis Research Center, Cleveland, OH, July 1988.

[6]Evans, D. S., private communication, GE Aircraft Engines, Cincinnati, OH, Aug. 1989.

[7]Levy, R., McDonald, H., Briley, W. R., and Kreskovsky, J. P., "Three-Dimensional Turbulent Compressible Subsonic Duct Flow Analysis for Use with Constructed Coordinate System," AIAA Paper 80-1398, July 1980.

[8]Levy, R., Briley, W. R., and McDonald, H., "Viscous Primary/Secondary Flow Analysis for Use with Nonorthogonal Coordinate Systems," AIAA Paper 83-0556, Jan. 1983.

[9]Briley, W. R., "Numerical Method for Predicting Three-Dimensional Steady Viscous Flow in Ducts," *Computational Physics*, Vol. 14, No. 1, 1974, pp. 8–28.

[10]Briley, W. R., and McDonald, H., "Analysis and Computation of Viscous Subsonic Primary and Secondary Flows," AIAA Paper 79-1453, July 1979.

[11]Briley, W. R., Kreskovsky, J. P., and McDonald, H., "Computation of Three-Dimensional Viscous Flow in Straight and Curved Ducts," United Technologies Research Center Rept. R76-911841, Aug. 1976.

[12]Eisenman, P. R., Levy, R., McDonald, H., and Briley, W. R., "Development of a Three-Dimensional Turbulent Duct Flow Analysis," NASA CR-3029, Nov. 1978.

[13]Reyhner, T. A., and Flugge-Lotz, I., "The Interaction of a Shock Wave with a Laminar Boundary Layer," *International Journal of Non-Linear Mechanics*, Vol. 3, No. 2, 1968, pp. 172–199.

[14]Towne, C. E., and Anderson, B. H., "Numerical Simulation of Flows in Curved Diffuser with Cross-Sectional Transitioning Using a Three-Dimensional Viscous Analysis," AIAA Paper 81-0003, Jan. 1981.

[15]Towne, C. E., "Computation of Viscous Flow in Curved Ducts and Comparison with Experimental Data," AIAA Paper 84-0531, 1984.

[16]Taylor, A. M. K. P., Whitelaw, J. H., and Yianneskis, M., "Measurement of Laminar and Turbulent Flow in a Curved Duct with Thin Inlet Boundary Layers," NASA CR-3367, Jan. 1981.

[17]Taylor, A. M. K. P., Whitelaw, J. H., and Yianneskis, M., "Turbulent Flow in a Square-to-Round Transition," NASA CR-3447, July 1981.

[18]Taylor, A. M. K. P., Whitelaw, J. H., and Yianneskis, M., "Developing Flow in S-Shaped Ducts, Part I: Square Cross Section Ducts," NASA CR-3550, May 1982.

[19]Taylor, A. M. K. P., Whitelaw, J. H., and Yianneskis, M., "Developing Flow in S-Shaped Ducts, Part II: Circular Cross Section Ducts," NASA CR-3759, Feb. 1984.